ACKNOWLEDGMENTS

We wish to thank the cyclotron crew at the Karlsruhe Cyclotron for their efforts during the irradiations.

[1]D. A. Orth, University of California Radiation Laboratory Report No. UCRL-1059, 1951 (unpublished).
[2]T. D. Thomas, R. Vandenbosch, R. A. Glass, and G. T. Seaborg, Phys. Rev. 106, 1228 (1957).
[3]D. J. Gorman and F. Asaro, Phys. Rev. C 3, 746 (1971).
[4]K. A. Keller, Radiochim. Acta 16, 138 (1971).
[5]F. L. Moore and J. E. Hudgens, Jr., Anal. Chem. 29, 1767 (1957).
[6]M. Hollstein, Nucl. Instr. Methods 82, 249 (1970).
[7]U. Jäger, Kernforschungszentrum Karlsruhe Report No. KFK 1646, 1972 (unpublished).
[8]U. Jäger, H. Münzel, G. Pfennig, to be published.
[9]S. G. Nilsson, C. F. Tsang, A. Sobiczewski, Z. Szymanski, S. Wycech, C. Gustafson, I. -L. Lamm, P. Möller, and B. Nilsson, Nucl. Phys. A131, 1 (1969).
[10]I. Ahmad, University of California Radiation Laboratory Report No. UCRL-16888, 1966 (unpublished).
[11]C. M. Lederer, J. K. Poggenburg, F. Asaro, J. O. Rasmussen, and I. Perlman, Nucl. Phys. 84, 481 (1966).
[12]E. K. Hyde, I. Perlman, and G. T. Seaborg, *The Nuclear Properties of the Heavy Elements* (Prentice Hall, Englewood Cliffs, New Jersey, 1964), Vol. 1, Chap. 3.
[13]E. K. Hyde, I. Perlman, and G. T. Seaborg, *The Nuclear Properties of the Heavy Elements* (Prentice Hall, Englewood Cliffs, New Jersey, 1964), Vol. 2, Chap. 9.
[14]K. A. Keller and H. Münzel, Kernforschungszentrum Karlsruhe Report No. KFK 1059, 1969 (unpublished).
[15]H. Brysk and M. E. Rose, Oak Ridge National Laboratory Report No. ORNL-1830, 1955 (unpublished).
[16]A. H. Wapstra and N. B. Gove, Nucl. Data A9, 265 (1971).
[17]R. S. Hager and E. C. Seltzer, Nucl. Data A4, 1 (1968).
[18]O. Dragoun, H. C. Pauli, and F. Schmutzler, Nucl. Data A6(No. 3), 235 (1969).

PHYSICAL REVIEW C VOLUME 7, NUMBER 4 APRIL 1973

Level Structure of ^{102}Pd Investigated by $(\alpha, xn\,;\gamma)$ Reactions

P. C. Simms, R. Anderson, F. A. Rickey, G. Smith, R. M. Steffen, and J. R. Tesmer
*Tandem Accelerator Laboratory,*Purdue University, Lafayette, Indiana 47907*
(Received 25 September 1972)

Levels in ^{102}Pd have been investigated by utilizing the ^{99}Ru$(\alpha,n\,;\gamma)^{102}$Pd reaction. The basic measurements were γ-ray excitation functions, angular distributions, and γ-γ coincidences. All γ-ray measurements were performed with Ge(Li) detectors. The excitation functions were used to identify ^{102}Pd γ rays, and the coincidence measurements were used to construct a level scheme. Nuclear spins have been inferred from analysis of the angular distributions. The proposed level scheme contains 24 levels; the dominant γ-ray cascade connects states of spin 0^+, 2^+, 4^+, 6^+, 8^+, and 10^+.

I. INTRODUCTION

In recent years many nuclei in various regions of the Periodic Table have been found to exhibit level structures that are intermediate to the vibrational and rotational extremes. In addition to the nuclei in the classic deformed regions of the rare-earth nuclei ($A = 150$–180) and the transuranium nuclei ($A > 230$), a number of nuclei around $A \simeq 80$ (e.g., $^{72-78}_{34}$Se, $^{78-84}_{36}$Kr)[1,2] and neutron deficient nuclei around $A \approx 126$ (e.g., $^{114-126}_{52}$Te, $^{120-130}_{54}$Xe, $^{124-126}_{56}$Ba, $^{128-136}_{58}$Ce)[3-7] have level structures that are reminiscent of ground-state rotational bands (see Fig. 1). Quasirotational levels with spins up to 10 have been found in some of these nuclei (e.g., $^{76}_{34}$Se, $^{126}_{54}$Xe).

Deformed nuclei are, in general, expected in regions where the neutron *and* proton numbers are far from those that correspond to closed shells.[8] In Fig. 1 stable even-Z nuclei have been plotted in an $N - Z$ diagram. The closures of major shells are indicated by solid vertical and horizontal lines. The closure of the semishell at $N, Z = 40$ is indicated by a dotted line. Regions where rotational-like level structures have been observed are cross-hatched. From this plot it is clear that deformed nuclei are not unexpected near $A \simeq 80$ and in neutron deficient isotopes around $A \simeq 126$.[8] Since the closure of the semishell at $N, Z = 40$ is relatively weak, a possible deformed region may exist for $34 < Z < 46$ and $54 < N < 76$.

Quasirotational bands with spins up to 10 have in-

deed been reported in $^{92-96}_{42}$Mo and $^{94-104}_{44}$Ru isotopes.[9,10] In view of these considerations a systematic study of the structure of the excited states of the even-A $_{46}$Pd nuclei is of considerable interest.

The structure of nuclei in this mass region is generally interpreted as vibrational in nature. In fact, in some textbooks the even-A Pd nuclei are quoted as the prototypes of harmonic vibrators. That this description is not adequate for the even-A Pd nuclei is evidenced by the fact that the first excited 2^+ states of these nuclei have quadrupole moments[11] of the order $Q \cong -0.5$ b and that reasonably strong $M1$ admixtures, which are forbidden between purely vibrational states, have been observed in the $2^{+\prime} \rightarrow 2^+$ transitions.[12]

The present paper describes an investigation of the excited states of ^{102}Pd by means of $(\alpha, n;\gamma)$ and $(\alpha, 2n;\gamma)$ reactions. Similar work is in progress for other even-A Pd isotopes and will be reported later.

The (α, n) and $(\alpha, 2n)$ reactions have been used to populate and identify a large number of excited states of ^{102}Pd. The identification of the ^{102}Pd excited states was mainly based on a comparison of the excitation curves for (α, n) and $(\alpha, 2n)$ reactions on different isotopes of Ru. Extensive use of directional distribution measurements on the

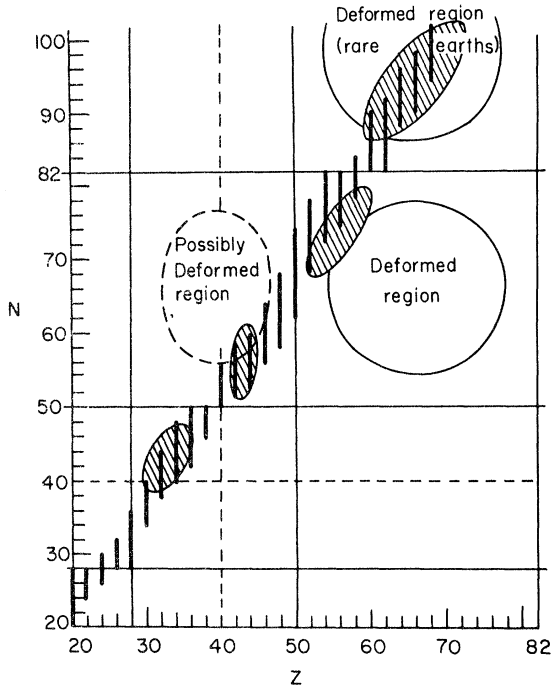

FIG. 1. N-Z diagram showing stable even-Z nuclei (heavy vertical bars), possible region of deformation, and regions where rotational-like structure has been observed (crosshatched areas).

γ rays emitted from the ^{102}Pd states and two-parameter γ-γ coincidence observations were used to establish a level scheme of up to 5-MeV excitation energy.

II. EXPERIMENTAL METHODS

The targets for the (α, xn) reaction experiments were made with enriched ^{99}Ru (98%) and ^{100}Ru (97%) metal obtained from Oak Ridge National Laboratory. Targets of approximately 100 μg/cm^2 thickness were evaporated from a cold crucible with heating obtained by electron bombardment of the Ru. The Ru condensed as a thin film on a 70-μg/cm^2 carbon backing.

The apparatus used for the excitation function and coincidence experiments consisted of a small aluminum target enclosure which allowed external detectors to be located within 2.5 cm of the beam spot. The beam was defined by tantalum collimators before the chamber and was collected in a Faraday cup 2 m behind the chamber. The chamber used in the angular-distribution measurements was a 12.7-cm-diam thin brass cylinder. A Ge(Li) detector could be rotated around the symmetry axis of the cylinder. The beam spot was fixed at the axis of rotation by a collimator with a 1.5-mm-diam hole located 20 cm in front of the target. An important test for an angular distribution is that it be symmetric around the beam axis. The chamber was not fitted with an exit beam line so that the γ detector could be positioned on both sides of the beam axis. The beam was stopped immediately behind the target with a 250-mg/cm^2 gold foil. The measurements that were performed for the determination of the beam spot location and for tests of the symmetry of the experimental arrangement will be described in Sec. V.

γ rays were detected with a Ge(Li) detector of 5% efficiency and 2-keV resolution at 1.3 MeV. The electronic system was designed to accept high counting rates and to provide a simple technique for corrections for dead-time and pileup losses. It was found that with proper pole-zero compensation and an active dc restorer the energy resolution did not deteriorate by more than 15% when the counting rate was increased from 5 to 30 kHz. Even though energy resolution need not suffer severely, pileup in the active filter amplifier is a serious problem for accurate measurements. The effect of pileup is to remove pulses from peaks and distribute them in the Compton background. In the present experiments the counting rates were typically 15 kHz, and the pileup loss was approximately 15%, quite comparable to the dead-time loss.

Dead-time and pileup losses were measured by using a pulser which was driven from the digital

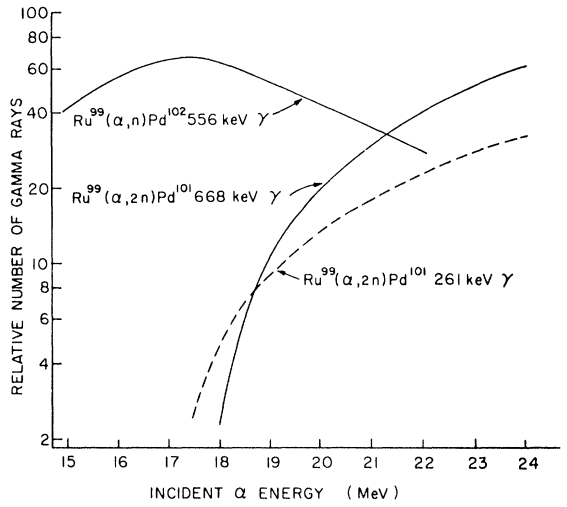

FIG. 2. Excitation functions for the 261-, 556-, and 668-keV γ rays observed in the ^{99}Ru(α, xn; γ) reaction.

output of the current integrator. The test pulse was carefully adjusted so that it would not cause undershoot in the active filter amplifier. The pulser-correction method was tested with sources of different strength and found to be accurate to within 0.3% for counting rates up to 30 kHz. The data were normalized by dividing the area of each γ-ray peak by the area of the pulser peak which was recorded in the upper part of the spectrum.

A time-to-amplitude converter was used for the γ-γ coincidence measurements to record true and chance coincidences simultaneously. The effective resolving time of the system was approximately 60 nsec, and the true-to-chance ratio was typically 30 to 1. The γ-γ coincidence spectra were recorded in a two-parameter analyzer-computer system with a 4096×4096 effective storage capability.

III. γ-RAY SPECTRA AND EXCITATION FUNCTIONS

For purposes of isotopic assignments of the γ rays the complete energy spectrum of the γ radiation emitted from the excited states populated in ($\alpha, xn;\gamma$) reactions from different Ru isotopes was measured with a high-resolution Ge(Li) detector as a function of the α energy. The γ detector was positioned at 90° with respect to the incident beam. A least-squares fit routine (GASPAN)[13] was used to decompose the γ spectrum into its components and the "excitation function" for each γ-ray energy was constructed. Figure 2 shows as an example the γ-ray yield as a function of α-particle energy for the first excited states of ^{102}Pd (from α, n) and ^{101}Pd (from $\alpha, 2n$). It is evident that at 17-MeV α energy the (α, n) reaction is dominant. At higher α energies the ($\alpha, 2n$) reaction becomes dominant[14] and more and more γ rays from ^{101}Pd produced in the ^{99}Ru($\alpha, 2n$)^{101}Pd reaction are observed. In fact, due to competition with the ($\alpha, 2n$) reaction the cross section for the (α, n) reaction peaks at E_α = 18 MeV and decreases at higher bombarding energies (see Fig. 2). Further confirmations for the assignments of the observed γ rays to transitions in ^{102}Pd were obtained by measuring the relative γ yields in the reaction ^{100}Ru($\alpha, xn;\gamma$)$^{104-x}$Pd as a function of α energy. In this case, the γ yield for ^{102}Pd γ rays increases constantly with increasing α energy and is expected to peak at about E_α = 26 MeV. The ^{100}Ru($\alpha, 2n;\gamma$)^{102}Pd reaction at E_α = 24 MeV resulted in the observation of the same ^{102}Pd γ rays as the ^{99}Ru($\alpha, n;\gamma$)^{102}Pd reaction. No additional γ rays were observed. In view of the considerable higher neutron and γ-ray background resulting from the ($\alpha, 2n$) reaction all the coincidence and directional distribution measurements which will be discussed in the following sections were made by using the ^{99}Ru($\alpha, n;\gamma$)^{102}Pd reaction at E_α = 17 MeV.

Table I summarizes the results of the excitation function measurements in the ^{99}Ru($\alpha, n;\gamma$)^{102}Pd reaction. Only those γ rays are included in the table that have been independently identified as originating in ^{102}Pd (see Sec. VI). The relative yields in Table I are corrected for the energy dependence of the counting efficiency of the Ge(Li) detector. All yields at $E_\alpha \neq 18$ MeV are normalized to the yield at E_α = 18 MeV. It is interesting to note that the yield for the 556-keV γ ray peaks at a lower α energy than the yield for the 835- and 979-keV γ rays, indicating that the latter γ rays are emitted from ^{102}Pd states of higher excitation energy.

IV. γ-γ COINCIDENCE MEASUREMENTS

γ-γ coincidence measurements were performed at an incident α energy of 17 MeV. The coincidence events were processed by two analog-to-digital converters (ADC) interfaced to a PDP-15 computer. The computer wrote the coincident word pairs on magnetic tape and accumulated a 4096 spectrum of all coincident events from ADC-A.

Data analysis was done off line. The computer was used to set windows on all peaks seen in the ADC-A spectrum. Since the windows also contained background caused by Compton scattering from higher-energy peaks, a background window was set adjacent to each peak window. Then a one-dimensional spectrum of ADC-B events was constructed for each ADC-A window. The background spectrum was subtracted from each peak spectrum.

The resultant spectrum for the 556-keV window is shown in Fig. 3. Peak areas and energies were extracted from each of these different coincidence spectra. The peak areas were then corrected for detector efficiency. A summary of the results of the coincidence measurement is given in Table II.

V. γ DIRECTIONAL DISTRIBUTION MEASUREMENTS

The directional distributions of the γ rays emitted from the excited states of ^{102}Pd populated in the ^{99}Ru$(\alpha, 2n)^{102}$Pd reaction at $E_\alpha = 17$ MeV were measured at laboratory angles of 90, 60, 30, 0, and $-30°$ with respect to the beam direction. After data were accumulated at each set of angles, a beam-off angular distribution of induced radioactivity in the target was measured. These radioactivity measurements were subsequently used to study the average effects of beam wobble and to determine the average position of the beam spot relative to the center of rotation of the Ge(Li) detector. Only the γ lines definitely identified as resulting from α-induced radioactivities were considered. After correcting for absorption in the stopping foil, the angular distributions of the radioactivity γ rays were found to be isotropic within 1%.

Three sets of data at a given angle were combined to give a mean normalized area for each γ transition observed. The rms deviation of the three areas from the mean was calculated to check the reproducibility of the data. Systematic errors in the measurements (beam centering, etc.) were estimated to contribute less than a 2% uncertainty. The statistical uncertainty, the rms deviation, and the systematic uncertainty were compared, and the largest uncertainty used in further calculations.

The resulting distributions were least-squares fitted to the function

$$N_\gamma(\theta) = N_0[1 + Q_2 A_{22} P_2(\cos(\theta - \theta_0)) + Q_4 A_{44} P_4(\cos(\theta - \theta_0))] \quad (1)$$

TABLE I. ^{99}Ru$(\alpha, n; \gamma)^{102}$Pd γ-ray yield as a function of incident α-particle energy.

E_γ (keV)	Intensity [b] at $E_\alpha = 18$ MeV	Intensity [a] as a function of E_α normalized to the intensity at $E_\alpha = 18$ MeV				
		16 MeV	17 MeV	18 MeV	19 MeV	20 MeV
179.8 ± 0.1	2.5	73 ± 1	99 ± 2	100 ± 2	89 ± 2	66 ± 2
182.9 ± 0.1	1.9	80 ± 2	95 ± 2	100 ± 2	82 ± 2	60 ± 2
275.1 ± 0.5	2.1	39 ± 2	56 ± 2	100 ± 3	126 ± 3	124 ± 3
327.3 ± 0.1	1.4	31 ± 2	64 ± 3	100 ± 4	125 ± 5	117 ± 5
336.2 ± 0.1	5.5	59 ± 1	82 ± 1	100 ± 1	88 ± 1	80 ± 1
440.0 ± 0.1	3.6	66 ± 2	89 ± 2	100 ± 2	91 ± 2	76 ± 2
540.0 ± 0.2	0.8	44 ± 7	57 ± 9	100 ± 15	193 ± 26	184 ± 23
556.4 ± 0.1	61.8	88 ± 0.3	105 ± 0.4	100 ± 0.4	82 ± 0.3	65 ± 0.3
603.6 ± 0.5	1.2	66 ± 8	86 ± 10	100 ± 12	67 ± 9	...
620.1 ± 0.5	2.0	85 ± 5	103 ± 6	100 ± 7	85 ± 6	93 ± 6
715.1 ± 0.5	8.4	...	...	100 ± 3	106 ± 3	84 ± 2
719.4 ± 0.1	47.4	77 ± 0.4	95 ± 0.5	100 ± 0.5	84 ± 0.5	67 ± 0.4
756.5 ± 1.0	1.4	55 ± 7	66 ± 7	100 ± 9	131 ± 11	108 ± 9
835.4 ± 0.2	23.3	61 ± 0.6	84 ± 0.8	100 ± 1	91 ± 1	77 ± 0.8
864.8 ± 1.0	2.9	75 ± 5	83 ± 6	100 ± 7	...	...
901.7 ± 0.1	9.1	44 ± 1	74 ± 2	100 ± 2	116 ± 2	113 ± 2
978.7 ± 0.5	3.5	72 ± 4	83 ± 4	100 ± 5	101 ± 5	96 ± 5
1018.4 ± 0.2	3.3	46 ± 3	95 ± 5	100 ± 5	118 ± 7	92 ± 6
1198.4 ± 0.2	2.5	54 ± 4	93 ± 6	100 ± 7	80 ± 6	57 ± 5
1277.7 ± 1.0	1.8	...	...	100 ± 12	80 ± 10	76 ± 10
1330.6 ± 0.5	1.5	83 ± 9	98 ± 11	100 ± 11	114 ± 14	138 ± 18
1375.4 ± 0.1	2.2	55 ± 5	81 ± 7	100 ± 8	82 ± 8	74 ± 7
1493.1 ± 0.3	1.8	109 ± 11	124 ± 12	100 ± 11	...	...
1554.9 ± 0.5	2.9	101 ± 6	116 ± 8	100 ± 7	103 ± 8	85 ± 7
1581.6 ± 0.1	5.7	70 ± 3	95 ± 4	100 ± 4	85 ± 4	65 ± 3
1745.1 ± 0.1	1.9	73 ± 8	99 ± 11	100 ± 11	78 ± 11	...
1786.5 ± 0.2	2.4	88 ± 9	85 ± 9	100 ± 12	...	...

[b] Relative intensity corrected for Ge(Li) detector efficiency.
[a] Normalized intensity × 100.

TABLE II. γ-γ coincidence summary. The γ rays listed in column I were selected on the A axis of the megachannel coincidence spectrum. The B detector spectra recorded in coincidence with the selected γ rays were then reconstructed. The energies of the γ rays seen in the B spectra are listed in column II. The intensities, given in parentheses, are corrected for the efficiencies of the Ge(Li) detectors.

E_γ (keV)	E_γ (keV)
327	184 (15±1.5), 556 (69±10), 719 (81±5), 835 (88±6), 902 (86±6)
336	176 (12±1.5), 221 (76±2), 275 (9±1.5), 440 (57±15), 556 (252±7), 604 (14±3), 719 (40±10), 715 (120±20), 757 (16±4), 835 (19±5), 861 (43±6), 900 (23±10), 978 (21±4), 1582 (193±13), 1534 (16±5)
440	180 (32±2), 275 (40±3), 336 (31±15), 556 (242±10), 719 (120±10), 757 (64±8), 1198 (20±6), 1582 (92±30)
556	180 (65±20), 183 (65±20), 275 (85±13), 327 (87±10), 336 (363±20), 383 (57±16), 440 (193±14), 719 (4416±80), 757 (61±22), 834 (1722±50), 861 (40±20), 865 (60±20), 890 (60±23), 902 (626±40), 979 (240±60), 1018 (400±60), 1198 (130±40), 1278 (100±40), 1331 (65±28), 1375 (153±35), 1493 (75±28), 1555 (301±37), 1582 (433±50), 1745 (164±31), 1787 (53±15)
719	180 (38±5), 256 (27±10), 327 (30±25), 336 (17±10), 440 (72±20), 541 (14±14), 556 (3712±110), 715 (96±30), 835 (1715±70), 865 (165±48), 890 (20±20), 901 (505±55), 979 (96±30), 1018 (212±35), 1198 (103±30), 1278 (29±13), 1331 (75±25), 1375 (138±30), 1493 (118±28)
835	183 (27±10), 327 (79±10), 336 (16±6), 540 (66±20), 556 (1620±40), 719 (1607±44), 865 (83±26), 890 (106±31), 902 (592±40), 979 (53±30)
902	327 (77±15), 556 (425±50), 719 (431±35), 835 (429±37), 978 (145±29)
979	383 (28±11), 556 (154±35), 719 (93±15), 835 (73±20), 902 (57±31)
1018	180 (29±5), 275 (10±4), 440 (18±5), 556 (170±61), 620 (19±5), 715 (93±15), 719 (230±22)
1198	275 (7±3), 383 (17±8), 440 (31±7), 556 (97±15), 714 (40±20), 719 (100±20)
1375	556 (110±22), 719 (106±16)
1493	556 (88±15), 719 (109±30)
1555	183 (54±6), 440 (16±7), 556 (183±19), 715 (27±12)
1582	275 (16±6), 336 (219±15), 440 (45±12), 556 (411±27), 714 (62±15)
1745	173 (10±4), 556 (127±15)

with N_0, A_{22}, A_{44}, and θ_0 as the parameters.

The corrections Q_i for finite solid angle were computed according to Krane.[15] The fits to the γ distributions were first made with θ_0 as a degree of freedom. The average θ_0 (about 2°) was then held fixed and the individual distributions analyzed again. The coefficients A_{22} and A_{44} with their respective uncertainties are tabulated in Table III for the ^{102}Pd γ rays. Figures 4 and 5 show some examples of the γ directional distribution measurements in the $(\alpha, n;\gamma)$ reactions.

VI. ANALYSIS AND INTERPRETATION OF THE DATA

A. Identification of γ Transitions

The γ rays observed in the singles spectra were identified as due to γ transitions in ^{102}Pd if the following conditions were met:

(a) peaking of yield at about $E_\alpha = 18$ MeV in the ^{99}Ru$(\alpha, n;\gamma)^{102}$Pd reaction,

(b) constant increase of the yield with increasing α energy up to $E_\alpha = 24$ MeV in the ^{100}Ru$(\alpha, 2n;\gamma)^{102}$Pd

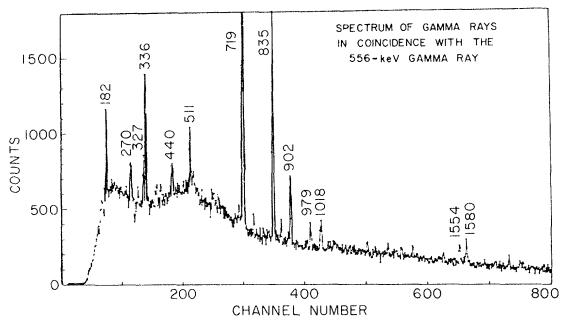

FIG. 3. Spectrum of γ rays detected in coincidence with the 556-keV γ ray.

reaction,
(c) coincidence events with γ rays that were firmly established to be ^{102}Pd transitions based on (a) and (b) alone.

B. Construction of Level Scheme of ^{102}Pd

After the determination of the relative intensities of the γ rays, the coincidence relationships between the various γ rays were analyzed on the basis of Table II. This table shows that several multiple γ cascades are present, the most prominent being the 556-719-835-902-979 chain, where the approximate energies are given in keV. (We define as a chain a set of γ rays where each γ ray of the set is in coincidence with every other member of the set.) The sequence of the γ chains are here written in order of ascending energies without regard, at this point, to the actual order of the γ rays in the decaying ^{102}Pd nucleus. Other rather prominent chains are the 275-336-440-556-1582, the 440-556-719-1198, and the 556-715-719-1198. It should be noted, however, that whereas some γ rays are members of several chains, they are not in coincidence with the *same* set of γ rays. For example, the 440-keV γ ray occurs in the first two sets, but the partners, 336 in the first set and 1198 in the second set, are *not* in coincidence with each other – a fact which indicates branching of the chain.

The observation that the 556-keV γ ray has a very strong coincidence probability with all γ transitions except with the 1534-keV γ ray, and the fact that the 556-keV transition is by far the most intense, clearly identifies it as the ground-state transition. This interpretation is borne out by the shape of the (α, xn) excitation function. The placement of the 556-keV γ ray is in agreement with the results from $(p, 2n)$ reactions on ^{103}Rh of Sakai, Yamazaki, and Ejiri[16] who observed the conversion electrons emitted in this transition and assigned an energy of 558 ± 3 keV to this γ ray.

The second most intense γ transition is the 719-keV transition, which is also in coincidence with most other transitions with the notable exception of the 1534-, 1582-, 1745-, and 1787-keV γ rays. It is therefore reasonable to place this transition on top of the 556-keV transition. Sakai, Yamazaki, and Ejiri[16] observed a 721 ± 3 keV γ ray following the ^{103}Rh$(p, 2n)^{102}$Pd reaction and interpreted this γ ray as due to the transition from the second to the first excited state of ^{102}Pd purely on the basis of systematics.

Similar coincidence and intensity considerations show that the 835-keV transition must be above the 719-keV transition. This γ transition was also identified by Sakai, Yamazaki, and Ejiri who quote as its energy $E_\gamma = (832 \pm 3)$ keV and place it above the 719-keV transitions on the basis of systematics.

From the coincidence data of Table II it follows that the 835-keV transition must be bypassed by the 1018-, 1198-, 1534-, 1555-, 1582-, 1745-,

TABLE III. Directional distributions of ^{102}Pd γ radiation emitted following the ^{99}Ru$(\alpha, n)^{102}$Pd reaction at $E_\alpha = 17$ MeV.

E_γ (keV)	$A_{22} \pm \Delta A_{22}$	$A_{44} \pm \Delta A_{44}$	E_γ (keV)	$A_{22} \pm \Delta A_{22}$	$A_{44} \pm \Delta A_{44}$
173	−0.23 ±0.03	0.105±0.011	865	−0.02 ±0.55	0.195±0.062
183	−0.19 ±0.02	0.103±0.03	902	0.313±0.016	−0.118±0.026
327	0.392±0.046	−0.019±0.073	979	0.158±0.026	−0.01 ±0.04
336	−0.167±0.026	0.045±0.040	1018	0.27 ±0.04	−0.07 ±0.09
440	0.345±0.035	−0.024±0.041	1198	−0.20 ±0.10	−0.004±0.110
556	0.199±0.018	−0.034±0.027	1278	−0.09 ±0.07	−0.13 ±0.106
604	0.31 ±0.09	−0.02 ±0.13	1331	−0.31 ±0.06	−0.09 ±0.08
620	0.03 ±0.04	+0.05 ±0.07	1375	0.23 ±0.05	0.01 ±0.07
715	0.116±0.025	−0.047±0.036	1493	−0.02 ±0.14	0.09 ±0.11
719	0.226±0.018	−0.047±0.028	1534	0.19 ±0.10	−0.14 ±0.17
757	0.38 ±0.06	0.03 ±0.09	1555	0.10 ±0.03	−0.04 ±0.05
835	0.277±0.018	−0.095±0.034	1582	0.23 ±0.02	−0.12 ±0.03
			1745	0.32 ±0.05	0.03 ±0.09

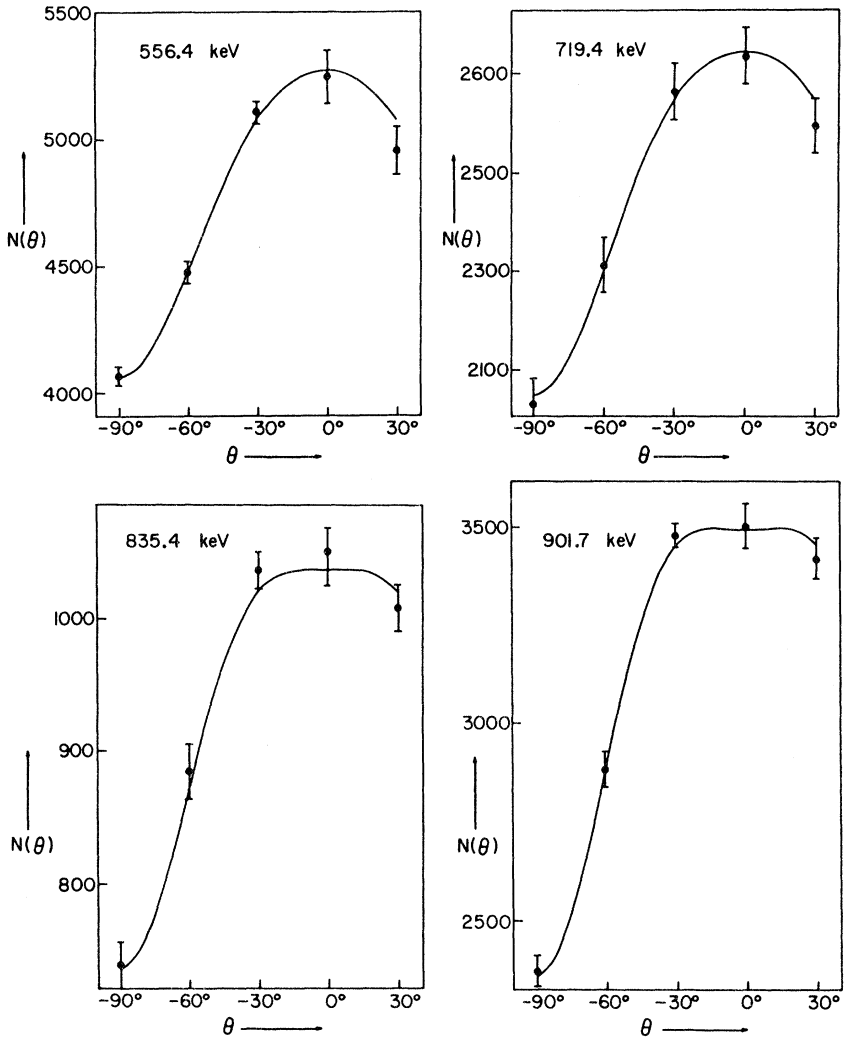

FIG. 4. Angular distributions and least-squares fits for the 556.4-, 719.4-, 835.4-, and 901.7-keV transitions.

and 1787-keV transitions.

From intensity and coincidence probability considerations it is clear that only some (about $\frac{1}{4}$) of the 978-keV quanta are in coincidence with the 835-keV transition. In fact, the width of the 978-keV γ peak in the singles spectrum indicates the presence of a doublet. Also, the excitation function for the 978-keV peak indicates that the peak is due to two different γ rays of about the same energy but placed at very different excitation energies.

A complete analysis of all the coincidence and intensity data, together with the accurate energy determination of the γ rays necessary for checking the presence of crossover transitions resulted in the level scheme shown in Fig. 6. By using the calibrated efficiency of the γ-γ coincidence detectors the coincidence intensities were computed on the basis of the level scheme of Fig. 6 and were found to be consistent with the experimental values of Table II.

C. Analysis of γ Directional Distribution Measurements

The $(\alpha, xn; \gamma)$ reactions proceed mainly through a compound nucleus mechanism. The incoming particle brings in orbital angular momentum in the $m = 0$ substate only with respect to the beam direction as the axis of quantization. The α particles with the energies involved in the present investigation bring into the compound system orbital angular momentum of up to 16 units, thus the compound nucleus is strongly aligned with respect to the beam direction. The neutrons evaporated from the compound nucleus before a particle-stable state is reached carry away small amounts of angular

momentum.[17] The angular momentum carried away by the neutrons is distributed in approximately random directions. γ radiations which may be emitted before the nuclear state under investigation is reached do not deorient the states appreciably. It is therefore reasonable to assume that the excited states of the Pd nuclei that are produced in the (α, xn) reaction are strongly aligned with a m-state population distribution $P(m)$ centered around $m=0$. The existence of the strong alignment was discovered by Morinaga *et al.*[18] and has been used as a spectroscopic tool in many investigations of $(\alpha, xn;\gamma)$ reactions.[18] We assume a Gaussian distribution of $P(m)$ with a width σ that depends on the details of the reaction mechanism[19]:

$$P(m) = e^{-m^2/2\sigma^2}. \tag{2}$$

The normalized ($B_0 = 1$) orientation parameters[20] of states of spin I are then given by

$$B_\lambda(I,\sigma) = (2I+1)^{1/2} \frac{\sum_{m=-I}^{+I} (-1)^{I+m} \langle I - mIm | \lambda 0 \rangle e^{-m^2/2\sigma^2}}{\sum_{m=-I}^{+I} e^{-m^2/2\sigma^2}} \tag{3}$$

and the directional distribution of γ radiation emitted from the aligned state I leading to a state I_f is given

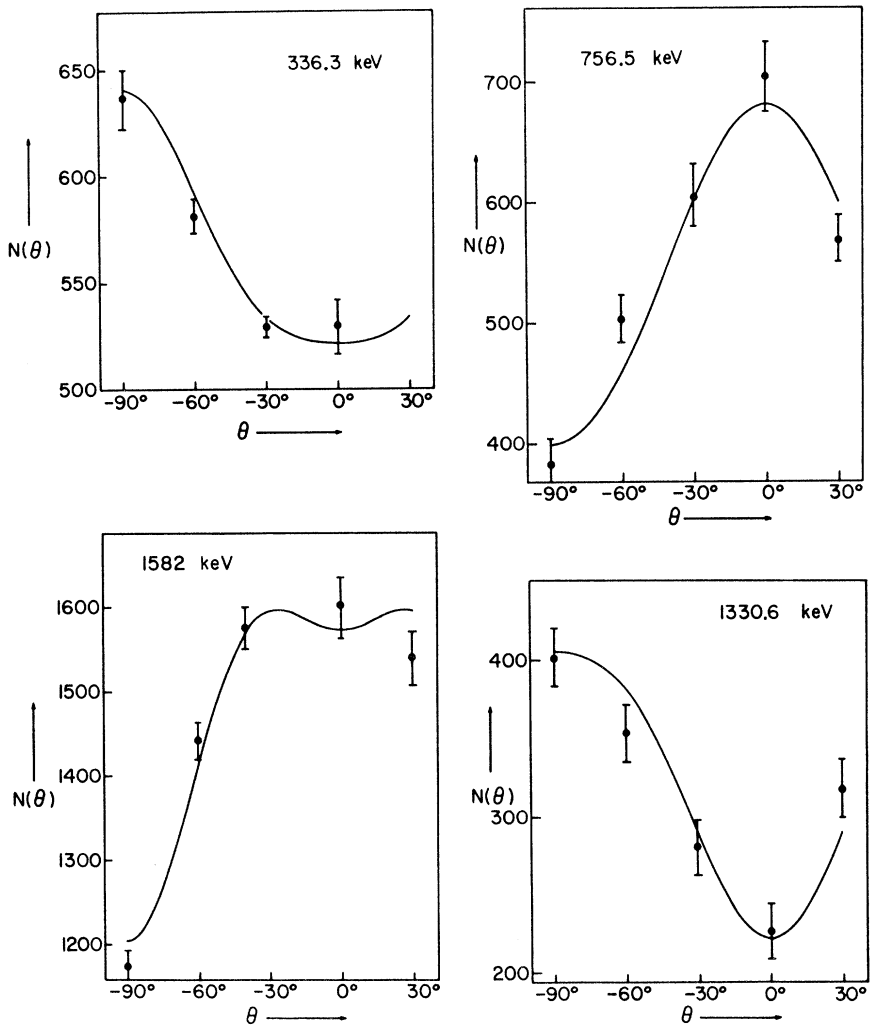

FIG. 5. Angular distributions and least-squares fits for the 336.3-, 756.5-, 1330.6-, and 1582-keV transitions.

by

$$W(\theta)=\sum_{\lambda} A_{\lambda\lambda} P_{\lambda}(\cos\theta) \tag{4}$$

with

$$A_{\lambda\lambda}=B_{\lambda}(I,\sigma)A_{\lambda}(\gamma)\,, \tag{5}$$

where the γ directional distribution coefficient $A_{\lambda}(\gamma)$ depends on the multipole character L of the γ transition. For a mixed L and L' γ transition

$$A_{\lambda}(\gamma)=\frac{F_{\lambda}(LLI_f I)+2\delta F_{\lambda}(LL'I_f I)+\delta^2 F_{\lambda}(L'L'I_f I)}{1+\delta^2}\,, \tag{6}$$

where the mixing ratio $\delta=\langle I_f\|\vec{j}_N\vec{A}_L^{(\pi)}\|I\rangle/\langle I_f\|\vec{j}_N\vec{A}_L^{(\pi)}\|I\rangle$ has been explicitly defined by Krane and Steffen.[21] For a pure multipole transition $L'=L$

$$A_{\lambda}(\gamma)=F_{\lambda}(LLI_f I)\,. \tag{7}$$

The factors $F_{\lambda}(LLI_f I)$ are the ordinary F coefficients.[22]

Figures 7 and 8 show the directional distribution coefficients

$$A_{\lambda\lambda}=B_{\lambda}(I,\sigma)F_{\lambda}(LLI_f I) \tag{8}$$

for quadrupole radiations $L=2$ and $I_f=I-2$ computed for various initial spins I as a function of the parameter σ/I.

It can be seen from Figs. 7 and 8 that the absolute values of the orientation parameters $B_{\lambda}(I,\sigma)$ decrease rapidly with increasing width σ of the m distribution and that $|B_4(I,\sigma)|$ decreases much faster than $|B_2(I,\sigma)|$.

It is convenient to introduce "attenuation" coefficients α_{λ} which describe the actually observed orientation parameters $B_{\lambda}(I)$ in terms of the orientation parameters $B_{\lambda}(I,0)$ for a perfect alignment with $\sigma=0$ (i.e., only population of $m=0$ substates):

$$\alpha_{\lambda}=\frac{B_{\lambda}(I)}{B_{\lambda}(I,0)}\,. \tag{9}$$

The α_{λ} are in general, smaller than unity, either because $\sigma\neq 0$ or because of the deorientation by virtue of the emission of a preceding radiation or because of both.

It is interesting to note that the attenuation coefficients for a state I whose orientation parameters $B_{\lambda}(I,\sigma)$ are given by Eq. (3) are nearly independent of I for $I>4$. Within a good approximation (a few percent) one can write

$$\alpha_{\lambda}(\sigma)\simeq\frac{B_{\lambda}(I,\sigma)}{B_{\lambda}(I,0)} \tag{10}$$

and the attenuation coefficients are then only a function of the relative spread σ/I. Figure 9 shows a plot of the $\alpha_2(\sigma)$ and $\alpha_4(\sigma)$ for $I=4$, 8, and 18 as a function of σ/I.

The orientation parameters of a state I_2 that is exclusively populated by an unobserved γ radiation γ_1 which has been emitted from a state I_1 with orientation parameters $B_{\lambda}(I_1)$, is given by

$$B_{\lambda}(I_2)=U_{\lambda\lambda}(\gamma_1)B_{\lambda}(I_1)\,, \tag{11}$$

where $U_{\lambda\lambda}(\gamma_1)$ is the deorientation coefficient[19] for the unobserved γ transition γ_1. The directional distribution of γ_2 is then given by

$$W(\theta)=\sum_{\lambda} B_{\lambda}(I_1)U_{\lambda\lambda}(\gamma_1)A_{\lambda}(\gamma_2)P_{\lambda}(\cos\theta)\,. \tag{12}$$

The directional distributions of γ rays in the 979-

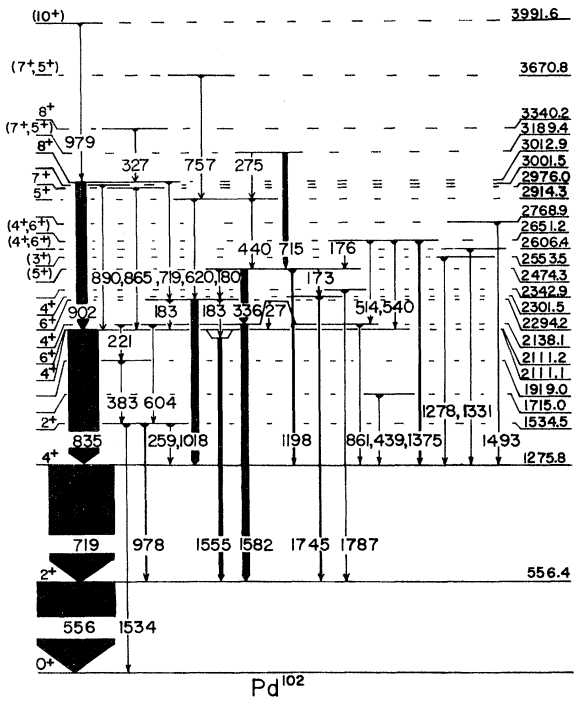

FIG. 6. Level scheme for ^{102}Pd.

902-835-719-556 chain (see Fig. 4) are discussed first. A summary of the directional distribution coefficients $A_{\lambda\lambda} = B_\lambda(I)A_\lambda(\gamma)$ observed for the γ rays in this chain is presented in Table V. The characteristic features of all these γ distributions are the relatively large and positive A_{22} values and the relatively small and negative A_{44} values. This feature is characteristic for $I \overset{L}{\rightarrow} I-2$ transitions.[19] The corresponding spin assignments to the nuclear states involved are indicated in column 4 of Table IV. The absence of crossover transitions corroborates these assignments. From the experimental $A_{\lambda\lambda}$ values the attenuation factors α_λ can be computed from Eq. (9). These factors are shown in columns 5 and 6 of Table IV. The corresponding magnetic substate spreads, σ/I obtained from Figs. 7 and 8 or 9 are indicated in columns 7 and 8 of Table IV.

Except for the 979-keV transition, which consists of two unresolved components, systematic trends in the α_λ's and the σ/I values are discernible. Within limits of error, the observed α_2 and α_4 values for a given state are consistent with Eq. (10) for a single value of σ/I. This fact implies that the analysis of the directional distribution data on the basis of a Gaussian distribution of the population parameters $P(m)$ following the (α, n) reaction is reasonable, albeit somewhat crude. As the γ cascade proceeds downwards, the α_λ decrease because of the emission of γ radiation (which deorients the nucleus).

If no side feeding is involved in a γ cascade, the reduction of α_λ can be computed from Eq. (11). For example, the 556-keV level is mainly fed by the 719-keV transition and hence its directional distribution is approximately given by Eq. (12) with[19] $U_{22} = 0.749$ and $U_{44} = 0.285$.

Hence, with Eqs. (8) and (9) and the experimental values of the $A_{\lambda\lambda}$ for the 719-keV transition, one expects $\alpha_2(556) = 0.33 \pm 0.03$ and $\alpha_4(556) = 0.034 \pm 0.021$ for the 556-keV transition, in excellent agreement with the experimental values. The argument can be reversed. The fact that the computed α_λ of the 556-keV state agree with the observed values indicates that the 556-keV state is mainly fed by the 719-keV transition, a result that is also obtained from intensity considerations.

The discussion above represents a special case of the general statement, that in a stretched cascade, i.e., a $I \overset{L}{\rightarrow} I - L \overset{L}{\rightarrow} I - 2L \overset{L}{\rightarrow} I - 3L \rightarrow$, etc. cascade with no side feeding, all γ rays must have the same directional distribution.[20] As can be seen from Table IV the 719 and 556 keV have within limits of error the same distribution, the 556-keV distribution being less pronounced than the 719-keV distribution because of some side feeding, In a similar way one can calculate from the $A_{\lambda\lambda}$ of the 835-keV transition the α_λ's for the 719-keV transition with the result $\alpha_2(719) = 0.55 \pm 0.04$ and $\alpha_4(719) = 0.26 \pm 0.09$. Here, the agreement is only qualitative, since the 1275.8-keV state is populated by many additional γ transitions, in fact less than half of the population is via the 835-keV transition.

These results show clearly that the dominant mode of deexcitation of the ^{102}Pd nuclei that are highly excited by (α, n) reactions is by means of a $(10) \rightarrow 8 \rightarrow 6 \rightarrow 4 \rightarrow 2 \rightarrow 0$ cascade. The spin assignments of 2^+ and 4^+ to the 556.4-keV and 1275.8-keV states agree with the results of the ^{103}Ru$(p, 2n)^{102}$Pd reaction work.[16]

The directional distribution of the γ rays emitted in the less intense chains are analyzed in Table V.

The 715-336-1582-556 cascade (see Fig. 6) is the second most intense chain in ^{102}Pd. The directional distribution of the 1582-keV γ ray (see Table V)

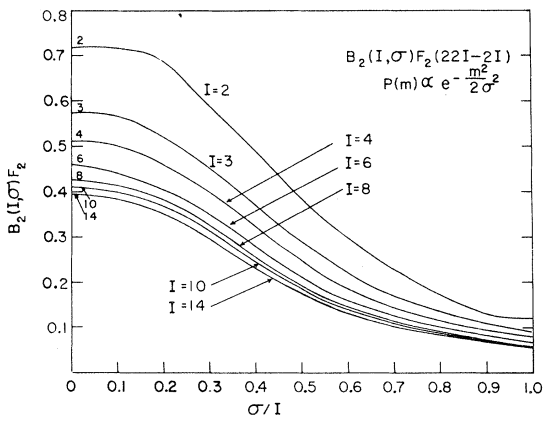

FIG. 7. Directional distribution coefficients $B_2(I,\sigma)F_2(2,2,I-2,I)$ as a function of σ/I for various values of I.

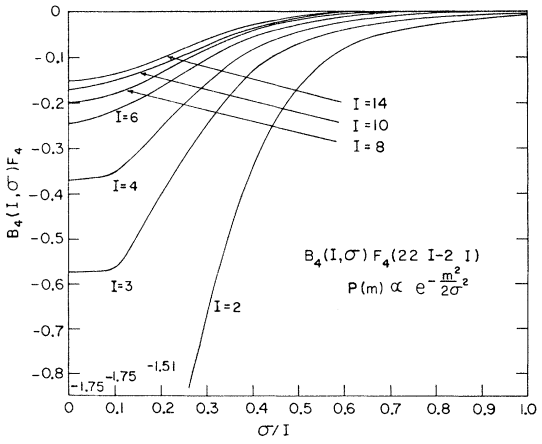

FIG. 8. Directional distribution coefficients $B_4(I,\sigma)F_4(2,2,I-2,I)$ as a function of σ/I for various values of I.

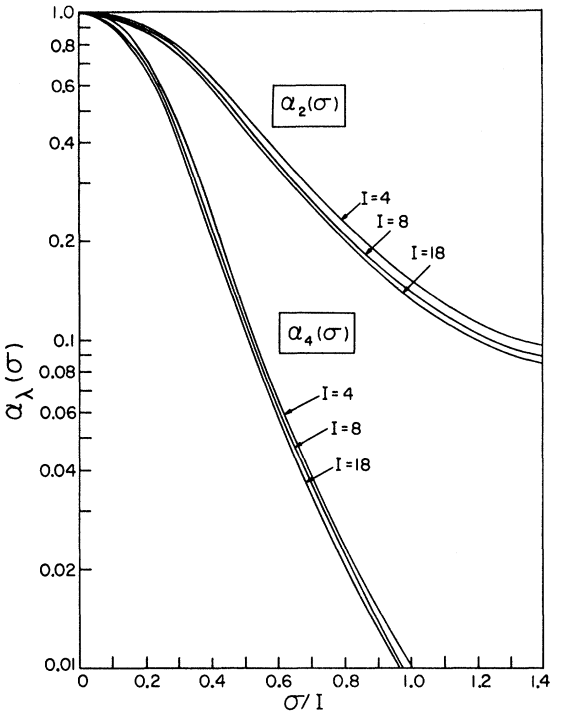

FIG. 9. Attenuation coefficients α_λ as a function of σ/I.

is characteristic of an $L=2$, $I_i=4\rightarrow I_f=2$ transition with $\alpha_2(1582)=0.45\pm0.04$ and $\alpha_4(1582)=0.33\pm0.08$. The σ/I values derived from $\alpha_2(1582)$ and $\alpha_4(1582)$, respectively, are not consistent with each other, but it should be kept in mind that this transition is mainly fed by the 336-keV transition. The directional distribution is consistent with either an $L=2$, $3\rightarrow4$ transition or an $L=1$, $5\rightarrow4$ transition. However, the $3\rightarrow4$ transition would result in α_λ's for the 1582-keV transition of $\alpha_2(1582)=\alpha_2(336)U_{22}(L=2)=0.26\pm0.06$ and $\alpha_4(1582)=\alpha_4(336)U_{44}(L=2)=-0.09\pm0.05$. [The negative sign here means that the orientation parameter $B_4(I=4)$ has an opposite sign to that of the initial state of the 336-keV transition. The original definition of the α_λ of Eq. (9) is still valid, but α_λ is here not a function of σ.] These values of $\alpha_\lambda(1582)$ are definitely not in agreement with the experimental values of Table V. If the 336-keV transition is interpreted as an $L=1$, $5\rightarrow4$ transition, however, one obtains $\alpha_2(1582)=\alpha_2(336)\,U_{22}(L=1)=0.47\pm0.07$, $\alpha_4(1582)=$no result, because A_{44} vanishes for $L=1$, in agreement with experiment. Also $U_{44}(L=1)=0.798$ which preserves a substantial part of any $\lambda=4$ orientation in the 336-keV transition, a fact which is important in explaining the experimental value of $\alpha_4(1582)=0.33\pm0.08$. The possible spin and multipole assignments for the 715-keV transition are indicated in Table V. The interpretation as a $7\rightarrow5$, $L=2$ transition cannot be excluded, but the small value of $\alpha_2(715)$ is unlikely for a state of spin 7. A more likely explanation of the observed distribution is based on the assumption that the 715-keV transition is a $5\rightarrow5$ transition of mixed multipolarity with a mixing ratio of $\delta=\langle5\|\vec{j}_N\vec{A}_2^{(E)}\|5\rangle/\langle5\|\vec{j}_N\vec{A}_1^{(M)}\|5\rangle=1.5$ (in the definition of Krane and Steffen).[21] This interpretation yields consistent and reasonable values for σ/I. The spin assignment of 5 to the initial state for the 336-keV transition, i.e., the 2474.3-keV state, fits in very well with the observed directional distribution of the 1198-keV γ ray which originates from the same state. The α_2's for both transitions agree within limits of errors. Similarly the observed directional distribution of the 440-keV transition is consistent with this assignment.

The 715-336-604-1534 cascade is of medium intensity. The 1582-keV and the 604-keV transition originate from the same state at 2138.1 keV. Both transitions are $4\rightarrow2$, $L=2$ transitions and the extracted values of α_2 and α_4 agree within experimental errors. The 1534.5-keV, $I=2^+$ state is mainly fed by the 604-keV transition, hence $\alpha(1534)=U_{22}(L=2)\,\alpha_2(604)=0.45\pm0.13$ in agreement with the data for the 1534-keV transition. The spin assignments of 4^+ to the 2138.1-keV and of 2^+ to the

TABLE IV. Directional distributions in the 979-902-835-719-556-keV chain.

E_γ (keV)	$A_{22}\pm\Delta A_{22}$	$A_{44}\pm\Delta A_{44}$	Transition $I_i\rightarrow I_f$	α_2	α_4	σ/I From α_2	σ/I From α_4
979[a]	0.158±0.026	−0.01 ±0.04	(10)→8				
902	0.313±0.016	−0.118±0.026	8→6	0.73±0.03	0.60 ±0.13	0.33±0.01	0.25±0.06
835	0.277±0.018	−0.095±0.034	6→4	0.61±0.04	0.39 ±0.14	0.41±0.01	0.32±0.09
719	0.226±0.018	−0.047±0.028	4→2	0.44±0.04	0.12 ±0.07	0.54±0.01	0.52±0.10
556	0.199±0.018	−0.034±0.027	2→0	0.27±0.04	0.020±0.014	0.75±0.01	$0.77^{+0.3}_{-0.10}$

[a] Composed of two γ rays of 978.7 and 978.1 keV.

TABLE V. Directional distributions in the 715-336-1582-556, the 715-1198-719-556, the 275-440-336-1582-556, the 715-336-604-1534, and the 757-620-1018-719-556 chain.

E_γ (keV)	$A_{22}\pm\Delta A_{22}$	$A_{44}\pm\Delta A_{44}$	Transition $I_i\rightarrow I_f$	L	α_2	α_4	σ/I From α_2	σ/I From α_4
715	0.116±0.025	−0.047±0.036	5→3	2	0.24±0.06	0.17±0.13	0.78±0.10	$0.45^{+0.24}_{-0.11}$
			7→5	2	0.25±0.07	0.22±0.16	0.76±0.12	$0.41^{+0.21}_{-0.09}$
			5→5	1,2 ($\delta=1.5$)	~0.5	~0.1	~0.5	~0.5
336	−0.167±0.026	+0.045±0.040	3→4	2	0.47±0.07	0.24±0.2	0.55±0.05	0.43±0.15
			5→4	1	0.50±0.08	···	0.48±0.07	···
1582	0.23 ±0.02	−0.12 ±0.03	4→2	2	0.45±0.04	0.33±0.08	0.53±0.03	0.35±0.05
1198	−0.20 ±0.10	0.00 ±0.11	3→4	2	0.56±0.28	<0.58	0.5 ±0.2	>0.26
			5→4	1	0.6 ±0.3	···	0.45±0.25	···
440	0.345±0.035	−0.024±0.041	5→3	2	0.73±0.05	<0.22	0.33±0.04	>0.41
			5→5	1	0.69±0.06	···	0.36±0.06	···
604	0.31 ±0.09	−0.02 ±0.13	4→2	2	0.61±0.18	0.06±0.24	0.42±0.14	>0.36
1534	0.19 ±0.10	−0.14 ±0.17	2→0	2	0.26±0.14	<0.18	$0.77^{+0.80}_{-0.16}$	>0.42
757	0.38 ±0.06	0.03 ±0.09	7→5	2	0.86±0.14	<0.28	$0.24^{+0.10}_{-0.24}$	>0.36
			5→5	1	0.76±0.08	···	0.30±0.05	···
620	0.03 ±0.04	0.05 ±0.07	5→6	1,2 ($\delta\cong-5.0$)	~0.7	~0.2	~0.35	~0.4
			5→6	1,2 ($\delta=-0.15$)	~0.7	0 to 1	~0.35	0 to ∞
1018	0.27 ±0.04	−0.07 ±0.09	6→4	2	0.59±0.09	<0.66	0.41±0.09	>0.2

TABLE VI. Directional distributions of the 327-, 865-, 1278-, 1331-, 1375-, 1493-, 1555-, and 1745-keV γ rays.

E_γ (keV)	$A_{22}\pm\Delta A_{22}$	$A_{44}\pm\Delta A_{44}$	Transition $I_i\rightarrow I_f$	L	α_2	α_4	σ/I From α_2	σ/I From α_4
173	−0.23±0.03	0.105±0.011	5→4	1, 2 ($\delta=-6.0$)	0.66±0.08	0.16±0.02	0.38±0.06	0.44±0.02
183[a]	−0.19±0.02	0.10 ±0.03	6→4	2				
183			6→6					
327	0.39±0.05	−0.02 ±0.07	8→8	1	0.78±0.10	···	0.30±0.07	···
865	−0.02±0.05	0.19 ±0.06	7→6	2	0 to 1	0.32±0.10	0 to ∞	0.34±0.06
1278	−0.09±0.07	0.13 ±0.11	3→4	2				
1331	−0.31±0.06	−0.09 ±0.08	4→4	2	0.8 to 1.0	0.15±0.13	0.0 to 0.3	0.5 ±0.3
1375	0.23±0.05	0.01 ±0.07	6→4	2	0.50±0.11	<0.25	0.47±0.07	>0.39
			4→4	1	0.46±0.10	···	0.42±0.07	···
1493	−0.02±0.14	0.09 ±0.11	4→4	1, 2 ($\delta=-0.6$)	~0.5	<0.15	~0.5	>0.45
1555	0.10±0.03	−0.04 ±0.05	4→2	2	0.20±0.05	$0.11^{+0.14}_{-0.11}$	0.86±0.10	$0.52^{+\infty}_{-0.12}$
1745	0.32±0.05	0.03 ±0.09	4→2	2	0.63±0.10	<0.16	0.40±0.06	>0.45

[a] There are two 183 γ rays. The observed $A_{\lambda\lambda}$ are consistent with the listed spin assignments which were derived from other transitions.

1534.5-keV state also agree with results from ^{102}Ag decay investigations.[23]

The 757-620-1018-719 cascade is a relatively weak chain, except for the 1018-keV transition which is strongly fed by high-energy γ rays following the (α, n) reaction. The 1018-keV transition, leading to the 1276-keV state with $I=4^+$, has a directional distribution that is characteristic for a $6 \rightarrow 4$, $L=2$ transition. The α_λ's and the σ/I values all indicate $I_i=6$ (compare with the 835-keV transition in Table IV). The absence of a cross-over transition to the 556.4-keV, $I=2^+$ state corroborates this interpretation. The interpretation of the practically isotropic distribution of the 620-keV γ radiation requires that this transition is a mixed $L=1$ and $L=2$ multipole with $\delta=-5.0$. The 757-keV transition is either an $L=1$, $5 \rightarrow 5$ or, more likely an $L=2$, $7 \rightarrow 5$ transition.

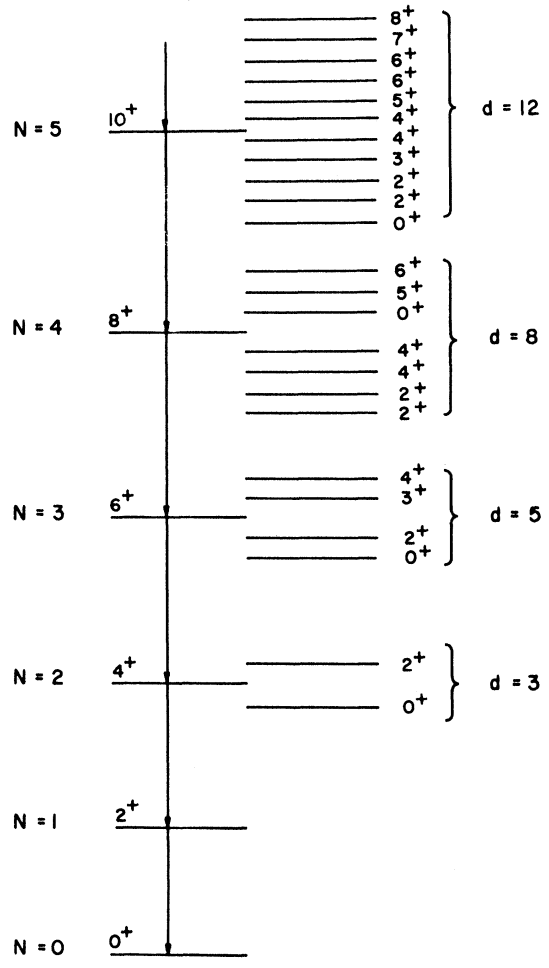

FIG. 10. Qualitative representation of vibrational states for multiplets with phonon numbers N up to $N=5$. Possible angular momenta are indicated. The ordering of angular momenta within a given multiple is arbitrary.

Table VI lists the directional distribution data and the interpretation of the remaining γ transitions which are not members of extensive chains. All these transitions are weak. It is interesting to note that the analysis of the data in Table VI gives consistent results in all cases where spin assignments have already been established on the basis of the earlier discussions.

VII. CONCLUSIONS

In the present work emphasis has been placed on producing states of high angular momentum in ^{102}Pd. States of low angular momentum are not easily populated in (heavy ion, xn) reactions. Thus in the interpretation of our results it must be remembered that many states with low angular momentum may be missing from the proposed level scheme.

In view of the strongly excited (10)-8-6-4-2-0 chain in ^{102}Pd the interpretation of these levels in terms of a quasirotational ground-state band is tempting. The energies of the excited states, however, are very different from the energies $E_I = (\hbar^2/2\mathcal{I}_0)I(I+1)$, predicted by the simple rotational model. Taking higher-order corrections into account Harris[24] generalized the simple rotational model and predicted the energies from the equations

$$E = \tfrac{1}{2}\omega^2(\mathcal{I}_0 + 3C\omega^2),$$

$$[I(I+1)]^{1/2} = \omega(\mathcal{I}_0 + 2C\omega^2).$$

Eliminating ω from these two equations, a cubic equation is obtained for E with $\mathcal{I}_0$ and C as parameters (variable moment of inertia model).[25] A least-squares fit to this equation for the observed energies of the ^{102}Pd "quasirotational" levels gives $\mathcal{I}_0 = 8.8\times10^{-6}$, $C = 6.22\times10^{6}$. In fact, if one sets $\mathcal{I}_0 = 0$ one obtains the simple equation

$$E_I = \text{const}\,[I(I+1)]^{2/3}$$

which gives a good fit for the energies of the ^{102}Pd "quasirotational" band.

The question arises, however, whether for a nucleus with $\mathcal{I}_0 \simeq 0$ it makes sense to talk about quasirotational levels, a concept which is based, in this case, entirely on the existence of a (10)-8-6-4-2-0 spin sequence. The quasirotational-band concept is particularly doubtful in the present case, where a very large number of states are present at low excitation energies besides the "quasirotational" levels.

A second approach is to interpret the excited states of ^{102}Pd in terms of a vibrational model, where the degeneracy of the phonon multiplets is removed by some additional interaction (slight anharmonicity, small rotational perturbation in the

higher phonon state, etc.). Figure 10 shows the angular momenta of the vibrational states for the various multiplets with phonon numbers N up to $N = 6$. A comparison of Fig. 10 with the level scheme of Fig. 6 shows a crude correspondence. The relatively large number of $I = 4^+$ and 6^+ states is easily understandable on the basis of the vibrational model. The absence of 0^+ states in the level scheme of ^{102}Pd is to be expected, because these levels are not populated in an (α, xn) reaction.

The strong (10)-8-6-4-2-0 chain is naturally explained by the fact that the ^{102}Pd nucleus in the (α, xn) reaction is produced in a high angular momentum state; hence, the deexcitation proceeds through the emission of γ rays which choose the highest angular momentum state available in each vibrational multiplet, giving the resemblance of a quasirotational cascade as far as angular momentum is concerned.

However, there are several problems with a vibrational interpretation. In a strictly vibrational nucleus $|\Delta N| \geq 2$ transitions are forbidden for $E2$ transitions; $M1$ transitions are forbidden for any ΔN. The existence of $\Delta N = 2$ transitions in ^{102}Pd, e.g., the 1534-, 1555-, 1582-, 1745-, and 1787-keV transitions, is a problem. Such crossover transitions do exist in many vibrational nuclei indicating that the vibrational picture is far from perfect. The regular energy spacing in the dominant chain cannot be explained.

The best description of ^{102}Pd may require a suitable microscopic model. Such a description may be very complicated. Many of the features of the level scheme, however, can be qualitatively understood by considering linear combinations of two-quasiparticle configurations. If the available shell-model orbits are limited to those in the $N = 5$ shell, the highest spin state allowed is a 10^+ state consisting of a pure $(h_{11/2})^2$ configuration. The relative number of 8^+, 7^+, 6^+, 5^+, and 4^+ states is also approximately correct. The strong (10)-8-6-4-2-0 chain might be understood as connecting states with strong $(h_{11/2})^2$ components. Specific calculations on ^{102}Pd have not been performed, but a simple microscopic model might be very useful.

At the present time it must be concluded that no simple model describes the states observed in ^{102}Pd. It seems to be neither strictly rotational nor vibrational. A more complete set of data is needed in order to make further conclusions. Nevertheless, it is obvious that this neutron-deficient Pd isotope exhibits many interesting properties, and merits further study.

---

*Work supported by the National Science Foundation.

[1]R. M. Lieder and J. E. Draper, Phys. Rev. C 2, 531 (1970).

[2]D. G. McCauley and J. E. Draper, Phys. Rev. C 4, 475 (1971).

[3]R. A. Warner and J. E. Draper, Phys. Rev. C 1, 1069 (1970).

[4]I. Bergström, C. J. Herrlander, A. Kerek, and A. Lukko, Nucl. Phys. A123, 99 (1969).

[5]A. Lukko, A. Kerek, I. Rezanka, and C. J. Herrlander, Nucl. Phys. A135, 49 (1969).

[6]J. E. Clarkson, R. M. Diamond, and F. S.Stephens, Nucl. Phys. A93, 272 (1967); D. Ward, F. S. Stephens, and R. M. Diamond, Nucl. Phys. A117, 309 (1968).

[7]G. L. Smith and J. E. Draper, Phys. Rev. C 1, 1548 (1970).

[8]R. K. Sheline *et al.*, Phys. Rev. Letters 7, 446 (1961).

[9]J. M. Jaklevic, C. M. Lederer, and J. M. Hollander, Phys. Letters 29B, 179 (1969); K. Hübenthal, E. Monnand, and A. Moussa, Nucl. Phys. A128, 577 (1969).

[10]F. K. McGowan, R. L. Robinson, P. H. Stelson, and W. T. Milner, Nucl. Phys. A113, 529 (1968); C. M. Lederer, J. M. Jaklevic, and J. M. Hollander, Nucl. Phys. A169, 449 (1971).

[11]W. R. Lutz, J. A. Thompson, R. P. Scharenberg, and R. D. Larsen, Phys. Rev. C 6, 1385 (1972).

[12]R. L Robinson, F. K. McGowan, P. H. Stelson, W. T. Milner, and R. O. Sayer, Nucl. Phys. A124, 553 (1969).

[13]Digital Equipment Corporation (unpublished).

[14]E. Bleuler, A. K. Stebbins, and D. J. Tendam, Phys. Rev. 90, 460 (1953).

[15]K. S. Krane, Nucl. Instr. Methods 98, 205 (1972).

[16]M. Sakai, T. Yamazaki, and H. Ejiri, Phys. Letters 12, 29 (1964); Nucl. Phys. 74, 81 (1965).

[17]J. O. Rasmussen and T. T. Sugihara, Phys. Rev. 151, 992 (1966).

[18]H. Morinaga and P. C. Gugelot, Nucl. Phys. 46, 210 (1963); H. Morinaga and N. Lark, Nucl. Phys. 67, 315 (1965); H. Morinaga, Nucl. Phys. 75, 385 (1966); N. Lark and H. Morinaga, Nucl. Phys. 63, 466 (1965).

[19]T. Yamazaki, Nucl. Data A3(No. 1), 1 (1967).

[20]R. M. Steffen and K. Alder, in *The Electromagnetic Interaction in Nuclear Physics*, edited by W. D. Hamilton (North-Holland, Amsterdam, 1972), Chap. XII.

[21]K. S. Krane and R. M. Steffen, Phys. Rev. C 2, 724 (1970).

[22]H. Frauenfelder and R. M. Steffen, in *Alpha-, Beta-, and Gamma-Ray Spectroscopy*, edited by K. Siegbahn (North-Holland, Amsterdam, 1965), p. 997.

[23]J. Liptak, J. Vrzal, E. P. Grigoriev, G. S. Katykhin, and J. Urbanec, Czech. J. Phys. 17B, 1127 (1969).

[24]S. M. Harris, Phys. Rev. 138, B509 (1965).

[25]M. A. J. Mariscotti, G. Scharff-Goldhaber, and B. Buck, Phys. Rev. 178, 1864 (1969).